Analysis of Hybrid PV Configurations to Mitigate Partial Shading Losses

Santosh B.S.S[*][‡] iD, Mohamed Thameem Ansari.M[*] iD, Kantarao.P[**] iD

Department of Electrical Engineering, Annamalai University and Annamalai Nagar 608002, India[*].

Department of Electrical Engineering, SRKREC and Bhimavaram, India[*].

Department of Electrical Engineering, Annamalai University and Annamalai Nagar 608002, India[**].

Department of Electrical Engineering, SRKREC and Bhimavaram, India[***].

(gangadharlakshmi555@gmail.com , ansariaueee@gmail.com, dr.pkantarao@gmail.com)

[‡]B.S.S. Santosh; gangadharlakshmi555@gmail.com

Abstract - In photovoltaic arrays, partial shadowing is the predominant issue. It has serious repercussions, including several maxima in electrical characteristics, hot spots on photovoltaic modules, disturbances in tracking maximum power, and diminished output power. During the majority of shadowing situations, the shade is concentrated in one section of the Photovoltaic (PV) array. This shade lowers the efficiency of the PV array. Combining PV modules in diverse configurations is one of the viable strategies for mitigating this issue. In this work, five hybrid configurations are analysed in the MATLAB/Simulink software. Each configuration's array voltage, array current, and array power values at each interval of bypass diode operation were calculated theoretically, and then compared with simulation results throughout a wide range of shade intensities.

Key words Partial Shading condition (PSC), Mismatch Power Loss, Hybrid PV array configurations, economic assessment.

1. Introduction

With the potential obsolescence of conventional energy sources in the near future, most nations have set long-term energy goals and plan to reduce their reliance on imports. This modern paradigm provides fresh insight into solar energy, in particular photovoltaic systems, which are favoured for electricity generation for a number of reasons [1]. From residential rooftop systems to massive utility-scale PV farms, solar power has been a rapidly expanding industry over the past decade. Solar power is a potentially lucrative source of renewable energy; hence, it is critical to evaluate the efficiency of solar photovoltaic (PV) systems [2]. PV module efficiency is affected by environmental conditions such as irradiance, temperature, humidity, wind velocity, orientation, and tilt angle. However, the arrays' maximum power generation is extremely dependent on the sun irradiation received and the module operating temperature. However, due to unanticipated losses brought on by the phenomenon of partial shading, the array's reliability and functionality are diminished. Partial shading occurs in a PV array when some modules are subjected to low irradiance levels because of the presence of unusual factors like shadow, leaves, dust, clouds,

or broken glass at the top of the modules. This circumstance creates mismatch between array modules and forces the entire PV array to deliver power equal to the lowest-performing modules [3]. Shading reduces photon current in PV cells. The generated photon current relies on PV cell area and irradiance, mismatching the surrounding fully lighted cells' current. Shaded cells may become reverse biased and behave as load, causing power loss. This causes hot-spot heating, which can cause permanent damage to the system if it is not adequately protected [4-6]. There are primarily two categories for partial shade mitigation, which are 1) passive mitigation solutions, such as bypass diodes and PV array topologies, and 2) active mitigation methods, such as MPPT approaches, and reconfiguration strategies. Despite low efficiency, these techniques have enabled the PV system to be used in several applications like commercial and residential buildings, electric vehicles, water pumping systems, etc. PV arrays have a single power maximum under homogeneous insolation. Multiple maxima are caused by bypass diodes [7], which are designed to eliminate hot spots when some modules receive less insulation. Traditional MPPT methods fare poorly in situations when there are many power maxima to be exist, such as in a partially shaded array or an array mounted on a

curved surface. P&O and IC are the most popular MPPT algorithms. Reasons include low cost, simplicity, and ability to track the MPP under uniform radiation conditions. Drawbacks include oscillations around the MPP and inefficiency under PSCs by confining to the nearest LMPP [8]. Various computational algorithm-based MPPT approaches, such as fuzzy control [9,10], neural network [11], particle swarm optimization (PSO) [12], etc., have shown good performance in tracking the global MPP. Each has limits. Most require experience configuring MPPT algorithm parameters and take a lengthy time to obtain global MPP. MPPTs based on computational algorithms use an iterative process to adjust the PV array's operating voltage according to the algorithm's updating strategy. These algorithms have slow tracking or premature convergence. Without shade, the PV system produces the same energy for all three converter methods in [13]. Under without bypass diode and shading situations, the micro-converter-based PV system produces the most energy. The micro converter-based PV system is expensive and can't prevent energy loss from shading. The study reveals that a central converter-based PV system with correctly built-in bypass diodes can improve efficiency, performance, and reliability [14]. examines various circuit topologies that explicitly mitigate the partial shading effects. However, these techniques suffer from high switching power loss, individual PV module failure to function at MPP, and a complex control framework. Various conventional array topologies have been presented in the literature in an effort to minimise mismatch losses. Conventional configurations are examined under six shading circumstances in [15]. Among all, TCT has the best maximum power, fill factor and least mismatch power loss under all shading circumstances. It concludes that PV array efficiency relies on configuration, solar irradiation, and shading position. For row, column, and diagonal shading patterns, [16] provides a mathematical representation of the TCT configuration and concludes that the superior performance of TCT is due to the greater number of internal connections between nodes in the TCT than in the SP, HC, or BL configurations, which provides more current paths and prevents current reduction in other branches. The performance of the various PV array topologies is evaluated in [17], and a mathematical study of the HC PV array architecture is provided as well. When the modules in the string were shaded together, the author found that the BLHC and TCT topologies were both at their best. BLHC is the best topology if the shade is uniform across all the strings. Depending on the shading intensity, SP, TCT, BLHC, or HC may be ideal if shaded modules cover half the strings. Shading on PV modules causes several output peaks, and the global maxima can be decreased when shaded modules are on the same location. When shaded modules are evenly distributed over different assemblies, the global peak is higher than local peaks [18]. Partial shading losses are not proportional to shaded area but rely on shading pattern, array arrangement, and module location [19]. Hence, the Magic Square-Enhanced Configuration (MS-EC) algorithm compares favourably with the existing techniques and a traditional Tied-Cross-Ties (TCT) configuration, giving average power improvements of 16–43% under most of the realistic weather conditions. Total-cross-tied (TCT)-based 'hybrid interconnection' schemes of solar PV array are investigated in [20] and author

concluded that proposed novel hybrid bridge-link (BL)-TCT and honey-comb (HC)-TCT interconnection schemes are found to be effective alternatives to achieve increased solar PV array output power. The simulation results indicate that the proposed 'hybrid interconnection' schemes with values of 17.5%, 21.28%, 54.33%, and 50.4% under four categories of typical PSC have the lowest MPL relatively compared to that of conventional interconnection schemes. From the literature, there is a chance to provide a complete mathematical analysis in terms of array voltage and array current equations at the time of changing their paths under changing shading conditions and also to assess the shading loss, misleading loss, and dispersion factor, which helps to identify the problems to reduce the difficulty of finding the global maximum power point.

The main aim of the paper is
1. Mathematical representation of hybrid topologies in partial shading.
2. Analyse hybrid topologies by operating panels, array voltage, array current, and array power at each string voltage interval.
3. Economics of hybrid configurations.

This paper is arranged as: Section 2 analyses Hybrid PV Array Configurations under one shading condition. Section 3 compares hybrid PV array configurations for different shading conditions, including performance and economic analysis. Finally, section 4 ends with conclusion.

2. Hybrid PV Configurations and Shading Patterns:

In this article, hybrid PV configurations are shown for analysis purposes. Various arrangements and shading techniques are depicted in Fig. 1. PV array configurations are modelled and simulated using a 6 by 6 matrix. For the MATLAB simulation, a SunPower SPR-76R-BLK-U PV module is used.

2.1 Numerical Representation of PV Configurations With Different Shading Patterns

The Unshaded module current, I_{USH} is expressed as I_{USH}
$$= I_L \times \frac{G}{G_{STC}} \approx I_{SC} \times \frac{G}{G_{STC}} \qquad (1)$$

Where I_L, G_{STC}: Photo current and Irradiance at Standard Test Conditions (STC) & $G_{STC} = 1000$ W/m²; G: Irradiance falling on the module under shading condition, I_{SC}: Short circuit current of the PV Module.

The Shaded module current, I_{SH} is expressed as
$$I_{SH} = I_L \times \frac{G_{SH}}{G_{STC}} = I_L \times \frac{(1-\beta)G}{G_{STC}} = I_{USH} - \left(\frac{G \times \beta}{G_{STC}} \times I_L\right) \qquad (2)$$

Where β: Shading factor and it is expressed as $\beta = 1 - \frac{G_{SH}}{G}$ and G_{SH}: Irradiance on shading condition

2.1.1 SP-TCT Configuration Under Uneven Row (UR) Shading Condition:

As can be seen in Fig. 1a, the first three rows of this particular interconnection scheme are connected in a Series Parallel (SP)

connection, while the following rows are connected in a total-cross-tied (TCT) form (1a). The shade condition in this arrangement affects Row -1 and Row -2 completely. From the equivalent circuit of PV module [13], the unshaded module current (I_A) and Shaded module current (I_B) are expressed as

$$I_A = I_{USH} - I_o \left[\exp\left(\frac{q \times V_{USH}}{nKT} \right) - 1 \right] \qquad (3)$$

Where,

(V, I) $_{USH}$ = Voltage & Currents of the Unshaded modules

$$= (V, I)_{3,9,15,21,27,33,4,10,16,22,28,34,5,11,17,23,29,35,6,12,18,24,30,36} \qquad (4)$$

Similarly, $I_B = I_{SH} - I_o \left[\exp\left(\frac{q \times V_{SH}}{nKT} \right) - 1 \right] \qquad (5)$

Where,

(V, I) $_{SH}$ = Voltage & Currents of the Shaded modules

$$= (V, I)_{1,7,13,19,25,31,2,8,14,20,26,32} \qquad (6)$$

From Fig. 1a, the array current (I_T) is expressed as,

$$I_T = I_I + I_{II} + I_{III} + I_{IV} + I_V + I_{VI} = I_4 + I_{10} + I_{16} + I_{22} + I_{28} + I_{34} \qquad (7)$$

Where $I_I = I_1 = I_2 = I_3$; $I_{II} = I_7 = I_8 = I_9$; $I_{III} = I_{13} = I_{14} = I_{15}$; $I_{IV} = I_{19} = I_{20} = I_{21}$; $I_V = I_{25} = I_{26} = I_{27}$; $I_{VI} = I_{31} = I_{32} = I_{33}$;

$$(8)$$

and

$I_4 = I_5 = I_6$; $I_{10} = I_{11} = I_{12}$; $I_{16} = I_{17} = I_{18}$; $I_{22} = I_{23} = I_{24}$; $I_{28} = I_{29} = I_{30}$; $I_{34} = I_{35} = I_{36}$;

$$(9)$$

From eqn (1), (2), (3) and (5)

$$I_T = I_I + I_{II} + I_{III} + I_{IV} + I_V + I_{VI}$$

$$= I_1 + I_7 + I_{13} + I_{19} + I_{25} + I_{31}$$

$$= 6I_B$$

$$= 6I_{SH} - 6I_o \left[\exp\left(\frac{q \times V_{SH}}{nKT} \right) - 1 \right]$$

$$= 6I_{USH} - 6\left(\frac{G \times \beta}{G_{STC}} \times I_L \right) - 6I_o \left[\exp\left(\frac{q \times V_{1,7,13,19,25,31}}{nKT} \right) - 1 \right]$$

$$= 6I_L \left(\frac{G}{G_{STC}} \right) - 6\left(\frac{G \times \beta}{G_{STC}} \times I_L \right) - 6I_o \left[\exp\left(\frac{q \times V_{1,7,13,19,25,31}}{nKT} \right) - 1 \right]$$

$$(10)$$

Similarly, from eqn (5),

$$I_T = 6I_L \left(\frac{G}{G_{STC}} \right) - 6I_o \left[\exp\left(\frac{q \times V_{4,10,16,22,28,34}}{nKT} \right) - 1 \right] \qquad (11)$$

Then $V_{3,4,5,6} = \frac{nKT}{q} \times \ln \left[\frac{6I_L\left(\frac{G}{G_{STC}} \right) - I_{4,5,6}}{6I_o} + 1 \right] \qquad (12)$

$$V_1 = V_2 = \frac{nKT}{q} \times \ln \left[\frac{6I_L\left(\frac{G}{G_{STC}} \right) - 6\left(\frac{G \times \beta}{G_{STC}} \times I_L \right) - I_I}{6I_o} + 1 \right] \qquad (13)$$

*2.1.2 BL-TCT Configuration Under Uneven Column (UC) Shading Condition:*

In this interconnection, the top three rows are Bridge-Link (BL) and the rest are total-cross-tied (TCT) as shown in Fig. 1b. In this configuration,

Column -1 and Column -2 are under shading condition. Where (V, I) $_{USH}$ = (V, I)$_{13,14,15,16,17,18,19,20,}$
$_{21,22,23,24,25,26,27,28,29,30,31,32,33,34,35,36}$ $\qquad (14)$

(V, I) $_{SH}$ = (V, I)$_{1,2,3,4,5,6,7,8,9,10,11,12}$ $\qquad (15)$

From Fig. 1b, the array current (I_T) is expressed as,

$$I_T = I_{XI} + I_{XII} + I_{XIII} + I_{XIV} + I_{XV} + I_{XVI} = I_4 + I_{10} + I_{16} + I_{22} + I_{28} + I_{34} \qquad (16)$$
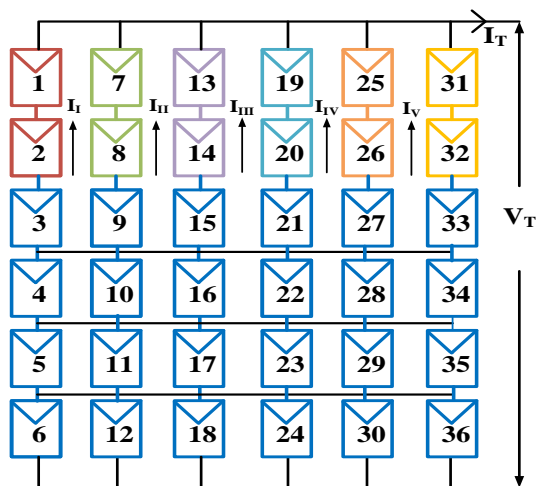
(a) SP-TCT: ROW SHADING
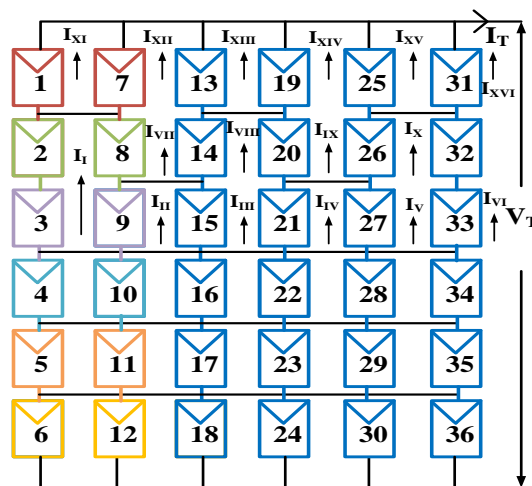
(b) BL-TCT: COLUMN SHADING
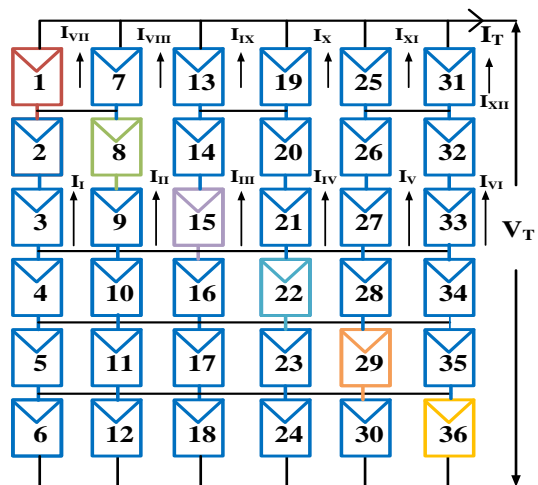
(c) HC-TCT: DIAGONAL SHADING
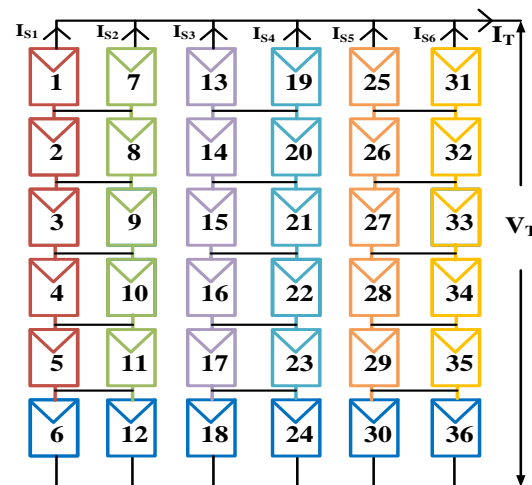
(d) ATCTSP: LONG WIDE SHADING
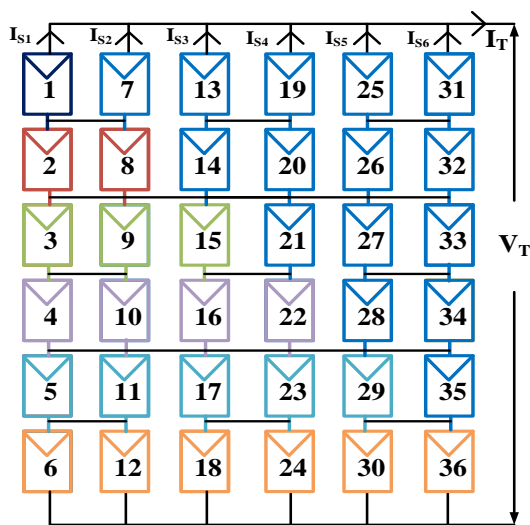
(e) ATCTBL: TRIANGULAR SHADING

(f) Shading Intensity on the modules

Fig. 1. Hybrid PV Array Configurations with different shading patterns

From equ (14), (15) and (16), the modified (I_T) is given as

$$I_T = 6I_L \left(\frac{G}{G_{STC}}\right) - 2\left(\frac{G \times \beta}{G_{STC}} \times I_L\right) - 2I_o\left[\exp\left(\frac{q \times V_{SH}}{nKT}\right) - 1\right] - 4I_o\left[\exp\left(\frac{q \times V_{USH}}{nKT}\right) - 1\right]$$

(17)

The array voltage (V_T) is expressed as,
$$V_T = V_1 + V_2 + V_3 + V_4 + V_5 + V_6 \tag{18}$$

The current through module – 1 can be expressed as
$$I_{XI} = I_L\left(\frac{G}{G_{STC}}\right) - \left(\frac{G \times \beta}{G_{STC}} \times I_L\right) - I_o\left[\exp\left(\frac{q \times V_1}{nKT}\right) - 1\right] \tag{19}$$

Then, voltage across module – 1 is,
$$V_1 = \frac{nKT}{q} \times \ln\left[\frac{I_L\left(\frac{G}{G_{STC}}\right) - \left(\frac{G \times \beta}{G_{STC}} \times I_L\right) - I_{XI}}{I_o} + 1\right] \tag{20}$$

Similarly,
$$V_2 = V_3 = \frac{nKT}{q} \times \ln\left[\frac{I_L\left(\frac{G}{G_{STC}}\right) - \left(\frac{G \times \beta}{G_{STC}} \times I_L\right) - I_I}{I_o} + 1\right] \tag{21}$$

$$V_{4,5,6} = \frac{nKT}{q} \times \ln\left[\frac{I_L\left(\frac{G}{G_{STC}}\right) - \left(\frac{G \times \beta}{G_{STC}} \times I_L\right) - I_{4,5,6}}{I_o} + 1\right] \tag{22}$$

2.1.3 HC-TCT configuration under Diagonal (DIA) shading condition:

In this interconnection scheme first three rows are connected in Honey Comb (HC) connection and remaining rows are connected in total – cross – tied (TCT) fashion. In this configuration, the modules in the diagonal position of the PV array are shaded as shown in the Fig. 1c. Where,

(V, I) $_{USH}$ = (V, I) $_{2,3,4,5,6,7,9,10,11,12,13,14,16,17,18,19,20,21,}$ $_{23,24,25,26,27,28,30,31,32,33,34,35}$ (23)
(V, I) $_{SH}$ = (V, I)$_{1,8,15,22,29,36}$ (24)

From Fig. 1c, the array current (I_T) is expressed as,
$$I_T = I_{VII} + I_{VIII} + I_{XI} + I_X + I_{XI} + I_{XII} = I_4 + I_{10} + I_{16} + I_{22} + I_{28} + I_{34} \tag{25}$$

From equ (23), (24) and (25), the modified (I_T) is given as
$$I_T = 6I_L\left(\frac{G}{G_{STC}}\right) - \left(\frac{G \times \beta}{G_{STC}} \times I_L\right) - 2I_o\left[\exp\left(\frac{q \times V_1}{nKT}\right) - 1\right] - 2I_o\left[\exp\left(\frac{q \times V_{13}}{nKT}\right) - 1\right] - 2I_o\left[\exp\left(\frac{q \times V_{25}}{nKT}\right) - 1\right] \tag{26}$$

And also
$$I_T = 6I_L\left(\frac{G}{G_{STC}}\right) - 6\left(\frac{G \times \beta}{G_{STC}} \times I_L\right) - 6I_o\left[\exp\left(\frac{q \times V_4}{nKT}\right) - 1\right] \tag{27}$$

From eqn (24) and (27),
$$V_{4,5,6} = \frac{nKT}{q} \times \ln\left[\frac{6I_L\left(\frac{G}{G_{STC}}\right) - \left(\frac{G \times \beta}{G_{STC}} \times I_L\right) - I_T}{I_o} + 1\right] \tag{28}$$

$$V_1 = \frac{nKT}{q} \times \ln\left[\frac{I_L\left(\frac{G}{G_{STC}}\right) - \left(\frac{G \times \beta}{G_{STC}} \times I_L\right) - I_1}{I_o} + 1\right] \tag{29}$$

Similarly,
$$V_2 = V_3 = \frac{nKT}{q} \times \ln\left[\frac{I_L\left(\frac{G}{G_{STC}}\right) - I_I}{I_o} + 1\right] \tag{30}$$

2.1.4 A-TCT-SP Configuration Under Long & Wide (LW) Shading Condition:

In this interconnection scheme first two columns are connected in total – cross – tied (TCT) fashion and second and third columns are in SP configuration alternatively as shown in the Fig. 1d with long and wide shading pattern.

Where   (V, I) $_{USH}$ = (V, I)$_{6,12,18,24,30,36}$ (31)
(V, I) $_{SH}$ = (V, I)$_{1,2,3,4,5,7,8,9,10,11,13,14,15,16,17,19,20,21,}$ $_{22,23,25,26,27,28,29,31,32,33,34,35}$ (32)

From Fig. 1d, the array current (I_T) is expressed as,
$$I_T = I_{S1} + I_{S2} + I_{S3} + I_{S4} + I_{S5} + I_{S6} \tag{33}$$
From eqn (3), (5), & (32), modified expression of I_T is given as,
$$I_T = 6I_L\left(\frac{G}{G_{STC}}\right) - 6\left(\frac{G \times \beta}{G_{STC}} \times I_L\right) - 2I_o\left[\exp\left(\frac{q \times V_1}{nKT}\right) - 1\right] - 2I_o\left[\exp\left(\frac{q \times V_{13}}{nKT}\right) - 1\right] - 2I_o\left[\exp\left(\frac{q \times V_{25}}{nKT}\right) - 1\right] \tag{34}$$

And also
$$I_T = 6I_L\left(\frac{G}{G_{STC}}\right) - 2I_o\left[\exp\left(\frac{q \times V_6}{nKT}\right) - 1\right] - 2I_o\left[\exp\left(\frac{q \times V_{12}}{nKT}\right) - 1\right] - 2I_o\left[\exp\left(\frac{q \times V_{30}}{nKT}\right) - 1\right] \tag{35}$$
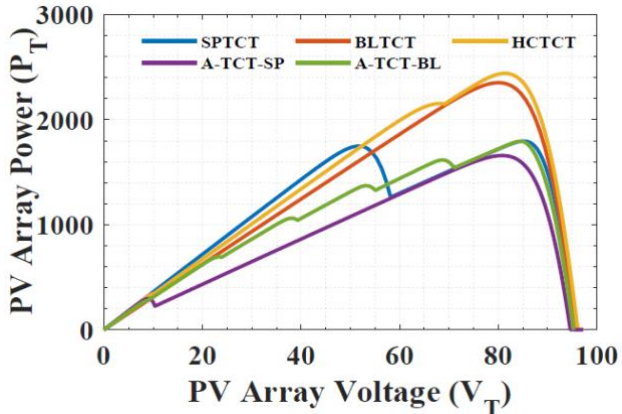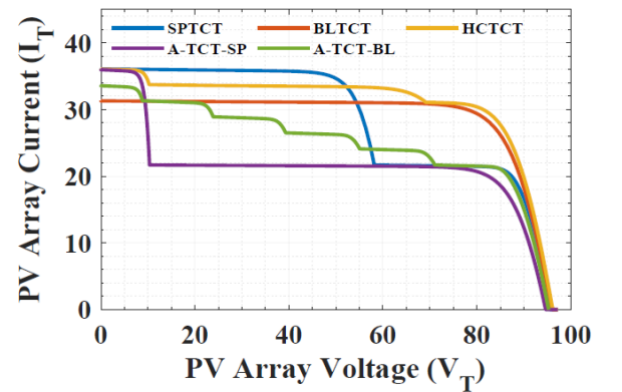

Fig. 2. Output characteristics of Hybrid PV Array Configurations for β = 0.4

Similarly

$$V_{1,2,3,4,5} = \frac{nKT}{q} \times \ln\left[\frac{I_L\left(\frac{G}{G_{STC}}\right)-\left(\frac{G\times\beta}{G_{STC}}\times I_L\right)-I_1}{I_o} + 1\right] \quad (36)$$

$$V_6 = \frac{nKT}{q} \times \ln\left[\frac{I_L\left(\frac{G}{G_{STC}}\right)-I_6}{I_o} + 1\right] \quad (37)$$

2.1.5 A-TCT-BL Configuration Under Triangular (TRI) Shading Condition:

In this interconnection scheme rows are alternatively connected in TCT and BL fashion as shown in the Fig. 1e with triangular shading pattern.

Where $(V, I)_{USH} = (V, I)_{7,13,19,25,31,14,20,26,32,21,27,33,28,34,35}$ (38)

$(V, I)_{SH} = (V, I)_{1,2,8,3,9,15,4,10,16,22,5,11,17,23,29,6,12,18,24,30,36}$ (39)

From Fig. 1e, the array current (I_T) is expressed as,
$$I_T = I_{S1} + I_{S2} + I_{S3} + I_{S4} + I_{S5} + I_{S6} = I_1 + I_7 + I_{13} + I_{19} + I_{25} + I_{31} \quad (40)$$

Where $I_1 = I_2 = I_3 = I_4 = I_5 = I_6; I_7 = I_8 = I_9 = I_{10} = I_{11} = I_{12}; I_{13} = I_{14} = I_{15} = I_{16} = I_{17} = I_{18};$
$I_{19} = I_{20} = I_{21} = I_{22} = I_{23} = I_{24}; I_{25} = I_{26} = I_{27} = I_{28} = I_{29} = I_{30}; I_{31} = I_{32} = I_{33} = I_{34} = I_{35} = I_{36};$ (41)

From eqn (40) and (41), the array current for each row can be expressed as,

Row-1, $I_T = 6I_L\left(\frac{G}{G_{STC}}\right) - \left(\frac{G\times\beta}{G_{STC}} \times I_L\right) - I_o\left[\exp\left(\frac{q\times V_{SH}}{nKT}\right) - 1\right] - 5I_o\left[\exp\left(\frac{q\times V_{USH}}{nKT}\right) - 1\right]$ (42)

Row-2, $I_T = 6I_L\left(\frac{G}{G_{STC}}\right) - 2\left(\frac{G\times\beta}{G_{STC}} \times I_L\right) - 2I_o\left[\exp\left(\frac{q\times V_{SH}}{nKT}\right) - 1\right] - 4I_o\left[\exp\left(\frac{q\times V_{USH}}{nKT}\right) - 1\right]$ (43)

Row-3, $I_T = 6I_L\left(\frac{G}{G_{STC}}\right) - 3\left(\frac{G\times\beta}{G_{STC}} \times I_L\right) - 3I_o\left[\exp\left(\frac{q\times V_{SH}}{nKT}\right) - 1\right] - 3I_o\left[\exp\left(\frac{q\times V_{USH}}{nKT}\right) - 1\right]$ (44)

Row-4, $I_T = 6I_L\left(\frac{G}{G_{STC}}\right) - 4\left(\frac{G\times\beta}{G_{STC}} \times I_L\right) - 4I_o\left[\exp\left(\frac{q\times V_{SH}}{nKT}\right) - 1\right] - 2I_o\left[\exp\left(\frac{q\times V_{USH}}{nKT}\right) - 1\right]$ (45)

Row-5, $I_T = 6I_L\left(\frac{G}{G_{STC}}\right) - 5\left(\frac{G\times\beta}{G_{STC}} \times I_L\right) - 5I_o\left[\exp\left(\frac{q\times V_{SH}}{nKT}\right) - 1\right] - I_o\left[\exp\left(\frac{q\times V_{USH}}{nKT}\right) - 1\right]$ (46)

Row-6, $I_T = 6I_L\left(\frac{G}{G_{STC}}\right) - 6\left(\frac{G\times\beta}{G_{STC}} \times I_L\right) - 6I_o\left[\exp\left(\frac{q\times V_{SH}}{nKT}\right) - 1\right]$ (47)

From eqn (42) – (47),

$$V_1 = \frac{nKT}{q} \times \ln\left[\frac{6I_L\left(\frac{G}{G_{STC}}\right)-\left(\frac{G\times\beta}{G_{STC}}\times I_L\right)-I_T}{6I_o} + 1\right] \quad (48)$$

$$V_2 = \frac{nKT}{q} \times \ln\left[\frac{6I_L\left(\frac{G}{G_{STC}}\right)-2\left(\frac{G\times\beta}{G_{STC}}\times I_L\right)-I_T}{6I_o} + 1\right] \quad (49)$$

$$V_3 = \frac{nKT}{q} \times \ln\left[\frac{6I_L\left(\frac{G}{G_{STC}}\right)-3\left(\frac{G\times\beta}{G_{STC}}\times I_L\right)-I_T}{6I_o} + 1\right] \quad (50)$$

$$V_4 = \frac{nKT}{q} \times \ln\left[\frac{6I_L\left(\frac{G}{G_{STC}}\right)-4\left(\frac{G\times\beta}{G_{STC}}\times I_L\right)-I_T}{6I_o} + 1\right] \quad (51)$$

$$V_5 = \frac{nKT}{q} \times \ln\left[\frac{6I_L\left(\frac{G}{G_{STC}}\right)-5\left(\frac{G\times\beta}{G_{STC}}\times I_L\right)-I_T}{6I_o} + 1\right] \quad (52)$$

$$V_6 = \frac{nKT}{q} \times \ln\left[\frac{6I_L\left(\frac{G}{G_{STC}}\right)-6\left(\frac{G\times\beta}{G_{STC}}\times I_L\right)-I_T}{6I_o} + 1\right] \quad (53)$$

From the eqn (11-13), (17), (20-22), (26-30), (34-37), (42-53) the short circuit current (I_{sc}) and the point at which I-V curve change its path (I_{cp}), number of maximum values for β = 0.4 and G = 1000 W/m^2 are mentioned in Table -1 and simulated results are shown in Fig. 2.

Table 1. Numerical analysis results

Topology	Shading Pattern	I_{sc} (A)	I_{cp} (A)	Peaks
SPTCT	UR	$6I_{sc}$	$6I_{sc} - 6 β I_{sc}$	2
BLTCT	UC	$6I_{sc} - 2 β I_{sc}$	-	1
HCTCT	DIA	$6I_{sc}$	$6I_{sc} - β I_{sc}$ $6I_{sc} - 2 β I_{sc}$	3
A-TCT-SP	LW	$6I_{sc}$	$6I_{sc} - 6 β I_{sc}$	2
A-TCT-BL	TRI	$6I_{sc} - β I_{sc}$	$6I_{sc} - 2 β I_{sc}$ $6I_{sc} - 3 β I_{sc}$ $6I_{sc} - 4 β I_{sc}$ $6I_{sc} - 5 β I_{sc}$ $6I_{sc} - 6 β I_{sc}$	6

3. Assessment of PV Array Configurations With Simulation Results:

The MATLAB tool simulates all 6 x 6 PV Array Hybrid topologies under uniform light and 5 partial shade situations. In Table. [2-6], operating panels, peak voltage (Vp), peak current (Ip), and peak power (Pp) are presented for each hybrid configuration under all shading circumstances. The parameters [19],[21] are used for assessing the performance of all hybrid configurations as mentioned in Table. 7 and Table. 8. The output characteristics and comparative analysis is represented in Fig. 3, Fig. 4, Fig. 5, Fig. 6, Fig. 7 and Fig. 8 respectively.

Table 2. Array Voltage, Array Current and Array Power for SPTCT Topology

Shading Scheme	Interval at which Array Voltage, Current and Power change					
Uneven Row	$0 \leq V_T \leq 4V_P$			$4V_P \leq V_T \leq 6V_P$		
Working Panels	3-6,9-12,15-18,21-24,27-30,33-36			1-2,7-8,13-14,19-20,25-26,31-32		
V_T	4 V_P			6 V_P		
I_T	6 I_P			3.3 I_P		
P_T	**24 $V_P I_P$**			19.8 $V_P I_P$		
Uneven Column	$0 \leq V_T \leq V_P$	$V_P \leq V_T \leq 2V_P$	$2V_P \leq V_T \leq 3V_P$	$3V_P \leq V_T \leq 4V_P$	$4V_P \leq V_T \leq 5V_P$	$5V_P \leq V_T \leq 6V_P$
Working Panels	6,12,18,24,30,36	5,11,17,23,29,35	4,10,16,22,28,34	3,9,15,21,27,33,2,20,26,32,1,19,25,31	3,21,27,33,2,8,14,20,26,32,1,19,25,31	1,7,13,19,25,31 2,8,14,20,26,32 3,9,15,21,27,33
V_T	V_P	$2V_P$	3 V_P	4 V_P	5 V_P	6 V_P
I_T	5.6 I_P	5.4 I_P	5.2 I_P	5 I_P	4.7 I_P	4.6 I_P
P_T	5.6 $V_P I_P$	10.8 $V_P I_P$	15.6 $V_P I_P$	20 $V_P I_P$	23.5 $V_P I_P$	**27.6 $V_P I_P$**
Diagonal	$0 \leq V_T \leq 2V_P$		$2V_P \leq V_T \leq 3V_P$	$3V_P \leq V_T \leq 4V_P$	$4V_P \leq V_T \leq 5V_P$	$5V_P \leq V_T \leq 6V_P$
Working Panels	7,13,19,25,31, 2,14,20,26,32, 3,9,21,27,33		19,25,31,20, 26,32,21,27, 33,6,12,18,2 4,30,36	19,25,31,20,26,32 ,21,27,33,5,11,17, 23,29,35	19,25,31,20,26 ,32,21,27,33,4, 10,16,22,28,34	1,7,13,19,25,31 2,8,14,20,26,32 3,9,15,21,27,33
V_T	$2V_P$		3 V_P	4 V_P	5 V_P	6 V_P
I_T	6 I_P		5.8 I_P	5.7 I_P	5.6 I_P	4.2 I_P
P_T	12 $V_P I_P$		17.4 $V_P I_P$	22.8 $V_P I_P$	**28 $V_P I_P$**	25.2 $V_P I_P$
Long & Wide	$0 \leq V_T \leq V_P$			$V_P \leq V_T \leq 6V_P$		
Working Panels	6,12,18,24,30,36			1-5,7-11,13-17,19-23,25-29,31-35		
V_T	V_P			6 V_P		
I_T	6 I_P			3.3 I_P		
P_T	6 $V_P I_P$			**19.8 $V_P I_P$**		
Triangular	$0 \leq V_T \leq V_P$	$V_P \leq V_T \leq 2V_P$	$2V_P \leq V_T \leq 3V_P$	$3V_P \leq V_T \leq 5V_P$		$5V_P \leq V_T \leq 6V_P$
Working Panels	7,13,19,25,31 14,20,26,32, 3,21,27,33	7,13,19,25,31 2,14,20,26,32, 3,9,21,27,33	7,13,19,25,3 1 2,14,20,26,3 2, 3,9,21,27,33 6,12,18,24,3 0,36	1,19,25,31 2,20,26,32, 3,21,27,33 4,10,16,22,28,34 5,11,17,23,39,35		1,19,25,31 8,20,26,32 15,21,27,33 4,10,16,22,28,3 4 5,11,17,23,39,3 5
V_T	V_P	2 V_P	3V_P	5V_P		6V_P
I_T	5.4 I_P	4.7 I_P	4.2 I_P	4 I_P		3.3 I_P
P_T	5.4 $V_P I_P$	9.4 $V_P I_P$	12.6 $V_P I_P$	**20$V_P I_P$**		19.8 $V_P I_P$

Table 3. Array Voltage, Array Current and Array Power for BLTCT Topology

Shading Scheme	Interval at which Array Voltage, Current and Power change	
Uneven Row	$0 \leq V_T \leq 4V_P$	$4V_P \leq V_T \leq 6V_P$
Working Panels	3-6,9-12,15-18,21-24,27-30,33-36	1-2,7-8,13-14,19-20,25-26,31-32
V_T	4 V_P	6 V_P
I_T	6 I_P	3.3 I_P

P_T	$24\ V_P I_P$			$19.8\ V_P I_P$		
Uneven Column	$0 \leq V_T \leq V_P$	$V_P \leq V_T \leq 2V_P$	$2V_P \leq V_T \leq 3V_P$	$3V_P \leq V_T \leq 4V_P$	$4V_P \leq V_T \leq 5V_P$	$5V_P \leq V_T \leq 6V_P$
Working Panels	6,12,18,24,30,36	5,11,17,23,29,35	4,10,16,22,28,34	3,9,15,21,27,33,2,20,26,32,1,25,31	3,21,27,33,2,8,14,20,26,32,25,31	1,7,13,19,25,31 26,32,33
V_T	V_P	$2V_P$	$3\ V_P$	$4\ V_P$	$5\ V_P$	$6\ V_P$
I_T	$5.6\ I_P$	$5.4\ I_P$	$5.2\ I_P$	$5\ I_P$	$4.9\ I_P$	$4.6\ I_P$
P_T	$5.6\ V_P I_P$	$10.8\ V_P I_P$	$15.6\ V_P I_P$	$20\ V_P I_P$	$24.5\ V_P I_P$	**$27.6\ V_P I_P$**
Diagonal	$0 \leq V_T \leq V_P$	$V_P \leq V_T \leq 2V_P$	$2V_P \leq V_T \leq 3V_P$	$3V_P \leq V_T \leq 4V_P$	$4V_P \leq V_T \leq 5V_P$	$5V_P \leq V_T \leq 6V_P$
Working Panels	6,12,18,24,30,36	5,11,17,23,39,35	4,10,16,22,28,34	25,31,2,20,26,32, 3,9,15,21,27,33	13,19,25,31 2,8,14,20,26,32 3,21,27,33	1,7,13,19,25,31 14,20,26,32 21,27,33
V_T	V_P	$2\ V_P$	$3\ V_P$	$4\ V_P$	$5\ V_P$	$6\ V_P$
I_T	$5.8 I_P$	$5.7\ I_P$	$5.6\ I_P$	$5.5\ I_P$	$5.4\ I_P$	$5.3\ I_P$
P_T	$5.8 V_P I_P$	$11.4\ V_P I_P$	$16.8\ V_P I_P$	$22\ V_P I_P$	$27\ V_P I_P$	**$31.8\ V_P I_P$**
Long & Wide	$0 \leq V_T \leq V_P$			$V_P \leq V_T \leq 6V_P$		
Working Panels	6,12,18,24,30,36			1-5,7-11,13-17,19-23,25-29,31-35		
V_T	V_P			$6\ V_P$		
I_T	$6\ I_P$			$3.3\ I_P$		
P_T	$6\ V_P I_P$			**$19.8\ V_P I_P$**		
Triangular	$0 \leq V_T \leq V_P$	$V_P \leq V_T \leq 2V_P$	$2V_P \leq V_T \leq 3V_P$	$3V_P \leq V_T \leq 4V_P$	$4V_P \leq V_T \leq 6V_P$	
Working Panels	1,7,13,19,25,31 14,20,26,32 21,27,33	13,19,25,31 8,14,20,26,32, 3,21,27,33	25,31 20,26,32, 21,27,33 6,12,18,24,30,36	25,31 2,20,26,32, 9,15,21,27,33 6,12,18,24,30,36	2,20 9,15,21,27,33 4,10,16,22,28,34 5,11,17,23,39,35	
V_T	V_P	$2\ V_P$	$3V_P$	$4V_P$	$6V_P$	
I_T	$5.2\ I_P$	$4.7\ I_P$	$4.2\ I_P$	$4.1\ I_P$	$4\ I_P$	
P_T	$5.2\ V_P I_P$	$9.4\ V_P I_P$	$12.6\ V_P I_P$	$16.4\ V_P I_P$	**$24\ V_P I_P$**	

Table 4. Array Voltage, Array Current and Array Power for HCTCT Topology

Shading Scheme	Interval at which Array Voltage, Current and Power change					
Uneven Row	$0 \leq V_T \leq 4V_P$			$4V_P \leq V_T \leq 6V_P$		
Working Panels	3-6,9-12,15-18,21-24,27-30,33-36			1-2,7-8,13-14,19-20,25-26,31-32		
V_T	$4\ V_P$			$6\ V_P$		
I_T	$6\ I_P$			$3.3\ I_P$		
P_T	**$24\ V_P I_P$**			$19.8\ V_P I_P$		
Uneven Column	$0 \leq V_T \leq V_P$	$V_P \leq V_T \leq 2V_P$	$2V_P \leq V_T \leq 3V_P$	$3V_P \leq V_T \leq 4V_P$	$4V_P \leq V_T \leq 5V_P$	$5V_P \leq V_T \leq 6V_P$
Working Panels	6,12,18,24,30,36	5,11,17,23,29,35	4,10,16,22,28,34	3,9,15,21,27,33, 14,20,26,32 13,19,25,31	15,21,27,33 2,8,14,20,26,32 13,19,25,31	15,21,27,33 14,20,26,32 1,7,13,19,25,31
V_T	V_P	$2V_P$	$3\ V_P$	$4\ V_P$	$5\ V_P$	$6\ V_P$
I_T	$5.6\ I_P$	$5.4\ I_P$	$5.2\ I_P$	$5\ I_P$	$4.8\ I_P$	$4.6\ I_P$
P_T	$5.6\ V_P I_P$	$10.8\ V_P I_P$	$15.6\ V_P I_P$	$20\ V_P I_P$	$24\ V_P I_P$	**$27.6\ V_P I_P$**

Diagonal	$0 \leq V_T \leq V_P$	$V_P \leq V_T \leq 2V_P$	$2V_P \leq V_T \leq 3V_P$	$3V_P \leq V_T \leq 4V_P$	$4V_P \leq V_T \leq 5V_P$	$5V_P \leq V_T \leq 6V_P$
Working Panels	13,19,25,31 2,14,20,26,32 3,9,21,27,33	13,19,25,31 2,14,20,26,32 3,9,21,27,33 6,12,18,24,30,36	13,19,25,31 2,14,20,26,32 3,9,21,27,33 5,11,17,23,29,35	13,19,25,31 2,14,20,26,32 3,9,21,27,33 4,10,16,22,28,34	13,19,25,31 2,8,14,20,26,32 3,9,21,27,33	1,7,25,31 20,26,32 15,21,27,33
V_T	V_P	$2 V_P$	$3 V_P$	$4 V_P$	$5 V_P$	$6 V_P$
I_T	$6 I_P$	$5.8 I_P$	$5.7 I_P$	$5.6 I_P$	$5.4 I_P$	$5.3 I_P$
P_T	$6 V_P I_P$	$11.6 V_P I_P$	$17.1 V_P I_P$	$22.4 V_P I_P$	$27 V_P I_P$	**$31.8 V_P I_P$**
Long & Wide	$0 \leq V_T \leq V_P$			$V_P \leq V_T \leq 6V_P$		
Working Panels	6,12,18,24,30,36			1-5,7-11,13-17,19-23,25-29,31-35		
V_T	V_P			$6 V_P$		
I_T	$6 I_P$			$3.3 I_P$		
P_T	$6 V_P I_P$			**$19.8 V_P I_P$**		
Triangular	$0 \leq V_T \leq V_P$	$V_P \leq V_T \leq 2V_P$	$2V_P \leq V_T \leq 3V_P$	$3V_P \leq V_T \leq 6V_P$		
Working Panels	1,7,13,19,25,31 14,20,26,32 21,27,33	13,19,25,31 14,20,26,32 3,9,21,27,33	25,31 20,26,32, 21,27,33 6,12,18,24,30,36	25,31 2,8,20,26,32, 15,21,27,33 4,10,16,22,28,34 5,11,17,23,29,35		
V_T	V_P	$2 V_P$	$3V_P$	$6V_P$		
I_T	$5.2 I_P$	$4.8 I_P$	$4.2 I_P$	$4 I_P$		
P_T	$5.2 V_P I_P$	$9.6 V_P I_P$	$12.6 V_P I_P$	**$24 V_P I_P$**		

Table 5. Array Voltage, Array Current and Array Power for ATCTSP Topology

Shading Scheme	Interval at which Array Voltage, Current and Power change					
Uneven Row	$0 \leq V_T \leq 4V_P$			$4V_P \leq V_T \leq 6V_P$		
Working Panels	3-6,9-12,15-18,21-24,27-30,33-36			1-2,7-8,13-14,19-20,25-26,31-32		
V_T	$4 V_P$			$6 V_P$		
I_T	$6 I_P$			$3.3 I_P$		
P_T	**$24 V_P I_P$**			$19.8 V_P I_P$		
Uneven Column	$0 \leq V_T \leq V_P$	$V_P \leq V_T \leq 2V_P$	$2V_P \leq V_T \leq 3V_P$	$3V_P \leq V_T \leq 4V_P$	$4V_P \leq V_T \leq 5V_P$	$5V_P \leq V_T \leq 6V_P$
Working Panels	6,12, 13-36	5,11, 13-36	4,10, 13-36	3,9, 13-36	2,8, 13-3631	1,7,13-36
V_T	V_P	$2V_P$	$3 V_P$	$4 V_P$	$5 V_P$	$6 V_P$
I_T	$5.6 I_P$	$5.4 I_P$	$5.2 I_P$	$5 I_P$	$4.8 I_P$	$4.6 I_P$
P_T	$5.6 V_P I_P$	$10.8 V_P I_P$	$15.6 V_P I_P$	$20 V_P I_P$	$24 V_P I_P$	**$27.6 V_P I_P$**
Diagonal	$0 \leq V_T \leq 4V_P$				$4V_P \leq V_T \leq 5V_P$	$5V_P \leq V_T \leq 6V_P$
Working Panels	13,19,25,31,14,20,26,32,3,9,27,33,4,10,28,34,5,11,17,23,6,12,18,24				2,8 16,22 30,36	1,7,13,19,25,31 14,20,26,32 21,27,33
V_T	$4 V_P$				$5 V_P$	$6 V_P$
I_T	$6 I_P$				$4.9 I_P$	$4.3 I_P$
P_T	$24 V_P I_P$				$24.5 V_P I_P$	**$25.8 V_P I_P$**
Long & Wide	$0 \leq V_T \leq V_P$			$V_P \leq V_T \leq 6V_P$		

Working Panels	6,12,18,24,30,36			1-5,7-11,13-17,19-23,25-29,31-35		
V_T	V_P			$6\,V_P$		
I_T	$6\,I_P$			$3.3\,I_P$		
P_T	$6\,V_P I_P$			**$19.8\,V_P I_P$**		
Triangular	$0 \leq V_T \leq V_P$	$V_P \leq V_T \leq 2V_P$	$2V_P \leq V_T \leq 3V_P$	$3V_P \leq V_T \leq 4V_P$	$4V_P \leq V_T \leq 5V_P$	$5V_P \leq V_T \leq 6V_P$
Working Panels	13,19,25,31 14,20,26,32 27,33 28,34 6,12	1,7,13,19,25,31 14,20,26,32 27,33 28,34 5,11	1,7,25,31 26,32 15,21,27,33 28,34 18,24	25,31 26,32 15,21 4,10 18,24	3,9 17,23 29,35	2,18 16,22 30,36
V_T	V_P	$2\,V_P$	$3V_P$	$4V_P$	$5V_P$	$6\,V_P$
I_T	$5.4\,I_P$	$5.2\,I_P$	$4.6\,I_P$	$4.4\,I_P$	$3.6\,I_P$	$3.2\,I_P$
P_T	$5.4\,V_P I_P$	$10.4\,V_P I_P$	$13.8\,V_P I_P$	$17.6\,V_P I_P$	$18\,V_P I_P$	**$19.2\,V_P I_P$**

Table 6. Array Voltage, Array Current and Array Power for ATCTBL Topology

Shading Scheme	Interval at which Array Voltage, Current and Power change					
Uneven Row	$0 \leq V_T \leq 4V_P$			$4V_P \leq V_T \leq 6V_P$		
Working Panels	3-6,9-12,15-18,21-24,27-30,33-36			1-2,7-8,13-14,19-20,25-26,31-32		
V_T	$4\,V_P$			$6\,V_P$		
I_T	$6\,I_P$			$3.3\,I_P$		
P_T	**$24\,V_P I_P$**			$19.8\,V_P I_P$		
Uneven Column	$0 \leq V_T \leq V_P$	$V_P \leq V_T \leq 2V_P$	$2V_P \leq V_T \leq 3V_P$	$3V_P \leq V_T \leq 4V_P$	$4V_P \leq V_T \leq 5V_P$	$5V_P \leq V_T \leq 6V_P$
Working Panels	17,23,29,35 6,12,18,24,30,36	5,11,17,23,29,35 18,24,30,36	15,21,27,33 4,10,16,22,28,34	3,9,15,21,27,33, 4,10,16,22,28,34	13,19,25,31 2,8,14,20,26,32	1,7,13,19,25,31 14,20,26,32
V_T	V_P	$2V_P$	$3\,V_P$	$4\,V_P$	$5\,V_P$	$6\,V_P$
I_T	$5.6\,I_P$	$5.4\,I_P$	$5.2\,I_P$	$5\,I_P$	$4.9\,I_P$	$4.6\,I_P$
P_T	$5.6\,V_P I_P$	$10.8\,V_P I_P$	$15.6\,V_P I_P$	$20\,V_P I_P$	$24.5\,V_P I_P$	**$27.6\,V_P I_P$**
Diagonal	$0 \leq V_T \leq V_P$	$V_P \leq V_T \leq 2V_P$	$2V_P \leq V_T \leq 3V_P$	$3V_P \leq V_T \leq 4V_P$	$4V_P \leq V_T \leq 5V_P$	$5V_P \leq V_T \leq 6V_P$
Working Panels	5,11,17,23 6,12,18,24,30,36	5,11,17,23,29,35 6,12,18,24,30,36	3,9,27,33 4,10,16,22,28,34	3,9,15,21,27,33 4,10,16,22,28,34	13,19,25,31 2,8,14,20,26,32 15,21	1,7,13,19,25,31 14,20,26,32
V_T	V_P	$2\,V_P$	$3\,V_P$	$4\,V_P$	$5\,V_P$	$6\,V_P$
I_T	$5.8\,I_P$	$5.7\,I_P$	$5.6\,I_P$	$5.5\,I_P$	$5.4\,I_P$	$5.3\,I_P$
P_T	$5.8V_P I_P$	$11.4\,V_P I_P$	$16.8\,V_P I_P$	$22\,V_P I_P$	$27\,V_P I_P$	**$31.8\,V_P I_P$**
Long & Wide	$0 \leq V_T \leq V_P$			$V_P \leq V_T \leq 6V_P$		
Working Panels	6,12,18,24,30,36			1-5,7-11,13-17,19-23,25-29,31-35		
V_T	V_P			$6\,V_P$		
I_T	$6\,I_P$			$3.3\,I_P$		
P_T	$6\,V_P I_P$			**$19.8\,V_P I_P$**		
Triangular	$0 \leq V_T \leq V_P$	$V_P \leq V_T \leq 2V_P$	$2V_P \leq V_T \leq 4V_P$		$4V_P \leq V_T \leq 6V_P$	
Working Panels	1,7,13,19,25,31 14,20,26,32	13,19,25,31 2,8,14,20,26,32,	15,21,27,33 4,10,28,34 29,35 6,12,18,24		3,9,27,33 16,22,28,34 5,11,17,23 30,36	

V_T	V_P	$2\,V_P$	$4V_P$	$6\,V_P$
I_T	$5.2\,I_P$	$4.6\,I_P$	$4.3\,I_P$	$3.8\,I_P$
P_T	$5.2\,V_P\,I_P$	$9.2\,V_P\,I_P$	$17.2\,V_P\,I_P$	**$22.8\,V_P\,I_P$**

Table 7. Global maxima, local maxima, Open circuit voltage and short circuit current of Hybrid PV configurations

Configuration	V_{oc} (V)	I_{sc} (A)	Global Values			Local Values		
			P_{mpp} (W)	V_{mpp} (V)	I_{mpp} (A)	P_{mpp} (W)	V_{mpp} (V)	I_{mpp} (A)
Un-Shading Scheme								
SPTCT	97.2	36.14	2746	81	33.87	--	--	---
BLTCT	97.2	36.14	2746	81	33.87	--	--	---
HCTCT	97.2	36.14	2746	81	33.87	--	--	---
ATCTSP	97.2	36.14	2746	81	33.87	--	--	---
ATCTBL	97.2	36.14	2746	81	33.87	--	--	---
Uneven Row (UR) Scheme								
SPTCT	96	36.13	1749	52	33.6	1632	85	19.25
BLTCT	96	36.13	1749	52	33.6	1648	85.34	19.32
HCTCT	96	36.13	1749	52	33.6	1665	86.4	19.26
ATCTSP	96	36.13	1749	52	33.6	1648	85.34	19.32
ATCTBL	96	36.13	1749	52	33.6	1655	85.85	19.26
Uneven Column (UC) Scheme								
SPTCT	95.3532	36.1	2180	81.648	26.6	262	8.0676	32.61
						697	21.87	31.94
						1122	36.7416	30.46
						1554	53.0712	29.2
						1947	68.9148	28.1
BLTCT	95.74	33.57	2188	81.84	26.87	261	8	32.7
						700	22	31.65
						1125	36.93	30.36
						1553	53.26	29
						1890	67.65	27.85
HCTCT	95.93	33.53	2180	81.93	26.52	233	7	33.21
						680	21.18	32
						1103	35.67	30.82
						1540	51.6	29.75
						1947	69	28.12
ATCTSP	96.13	33.66	2102	80.676	25.97	284	8.55	33.19
						753	23.42	32
						1209	39.17	30.77
						1638	51.61	29.44
						2019	71.63	28.1
ATCTBL	95.74	33.63	2200	82.1	26.7	299	9.234	32.38
						685	21.57	31.67
						1155	37.9	30.37
						1506	51.61	29.1
						1913	68	28.03
Diagonal Scheme (DIA)								
SPTCT	95.35	36.1	2187	67.068	32.41	794	22.5504	35
						1260	36.45	34.33
						1702	50.058	33.82
						2034	82.62	24.47
BLTCT	95.35	36.1	2480	80.38	30.68	230	6.6	34.47
						682	20	33.89
						1148	34.31	33.25
						1630	49.47	32.75
						2106	65.7	31.86
HCTCT	95.35	36.1	2307	82.4	27.81	324	9.13	35.35
						743	21.4	34.55

						1228	36	33.85
						1698	51	33.13
						2103	68.23	30.63
ATCTSP	95.64	36.1	2218	84	26.43	1749	51.51	33.74
						1944	69.88	27.65
ATCTBL	95.83	34.83	2484	80.67	30.6	280	8.06	34.44
						668	19.63	33.85
						1187	35.47	33.26
						1582	48.21	32.61
						2074	64.34	32.04
Long and Wide (LW) Scheme								
SPTCT	94.5756	35.93	1519	80.48	18.75	296	8.845	33.27
BLTCT	94.5756	35.93	1519	80.48	18.75	296	8.845	33.27
HCTCT	94.5756	35.93	1519	80.48	18.75	296	8.845	33.27
ATCTSP	94.5756	35.93	1519	80.48	18.75	296	8.845	33.27
ATCTBL	94.5756	35.93	1519	80.48	18.75	296	8.845	33.27
Triangular (TRI) Scheme								
SPTCT	94.5756	35.93	1804	80.48	22.2	299	9.81	30.33
						659	24.59	26.65
						977	39.65	24.5
						1600	68.23	23.35
BLTCT	94.5756	35.93	1863	80.38	23	285	9.62	29.45
						650	24.6	26.27
						960	38.6	24.73
						1191	49	24.16
HCTCT	95.06	31.23	1842	80.67	22.69	282	9.33	29.98
						663	24.3	27.13
						972	39.36	24.55
ATCTSP	95.54	32.74	1516	85	17.82	284	8.94	31.68
						720	24.78	30.03
						1046	38.88	26.82
						1326	52.48	25.26
						1471	69	21.26
ATCTBL	94.96	31.21	1813	81.65	22.07	284	9.52	29.61
						591	21.96	26.74
						1318	52	25.19

Table 8. Shading Loss, % Mismatch Loss, Mis-leading Loss, Fill Factor and Efficiency of Hybrid PV configurations

Topology	Total power in shading condition (W)	Unshaded maximum array power (W)	Shading Loss (W)	% Mismatch Loss	Mis-leading Loss (W)	Fill Factor	Input power (P_{in}) = Insolation × area	Efficiency =P_{mpp}/ P_{in}
Un Shading Scheme (UN)	---	2746	**---**	**---**	----	0.782	19440	14.12551
Uneven Row (UR) Scheme								
SPTCT	2329.69	2746	416.33	24.9	99	0.51	16524	10.58
BLTCT	2329.69	2746	416.33	24.9	99	0.51	16524	10.58
HCTCT	2329.69	2746	416.33	24.9	99	0.51	16524	10.58
ATCTSP	2329.69	2746	416.33	24.9	99	0.51	16524	10.58
ATCTBL	2329.69	2746	416.33	24.9	99	0.51	16524	10.58
Uneven Column (UC) Scheme								
SPTCT	2329.69	2746	416.33	6.42	233	0.63	16524	13.19
BLTCT	2329.69	2746	416.33	6.08	298	0.68	16524	13.24
HCTCT	2329.69	2746	416.33	6.42	233	0.67	16524	13.19

ATCTSP	2329.69	2746	416.33	9.77	83	0.64	16524	12.72
ATCTBL	2329.69	2746	416.33	5.56	287	0.68	16524	13.31
Diagonal (DIA) Scheme								
SPTCT	2537.88	2746	208.12	13.82	153	0.6	17982	12.16
BLTCT	2537.88	2746	208.12	2.2	376	0.71	17982	13.8
HCTCT	2537.88	2746	208.12	9.09	204	0.66	17982	12.82
ATCTSP	2537.88	2746	208.12	12.60	274	0.643	17982	12.33
ATCTBL	2537.88	2746	208.12	2.123	410	0.7	17982	13.81
Long-Wide (LW) Scheme								
SPTCT	1705.09	2746	1040.93	10.91	1222	0.444	12150	12.5
BLTCT	1705.09	2746	1040.93	10.91	1223	0.444	12150	12.5
HCTCT	1705.09	2746	1040.93	10.91	1223	0.444	12150	12.5
ATCTSP	1705.09	2746	1040.93	10.91	1223	0.444	12150	12.5
ATCTBL	1705.09	2747	1040.93	10.91	1223	0.444	12150	12.5
Triangular (TRI) Scheme								
SPTCT	1990.43	2746	755.57	9.36	204	0.52	14148	12.75
BLTCT	1990.43	2746	755.57	6.4	672	0.544	14148	13.16
HCTCT	1990.43	2746	755.57	7.45	870	0.61	14148	13.019
ATCTSP	1990.43	2746	755.57	23.83	45	0.484	14148	10.71
ATCTBL	1990.43	2746	755.57	8.91	495	0.608	14148	12.81
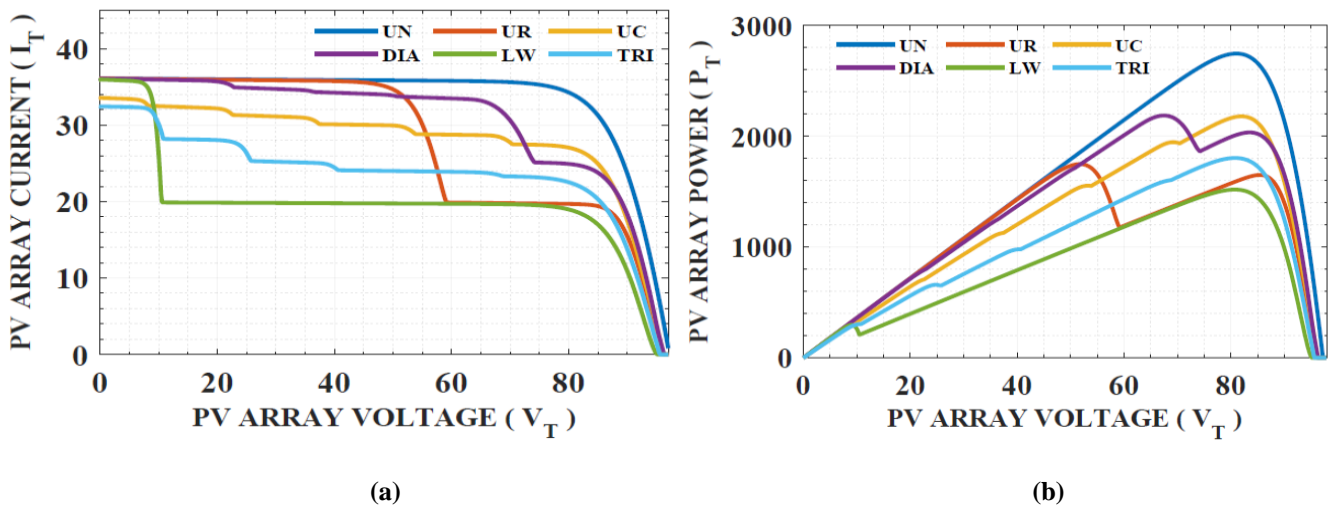
Fig. 3. (a) Array Current Curve (b) Array Power Curve of SPTCT Configuration
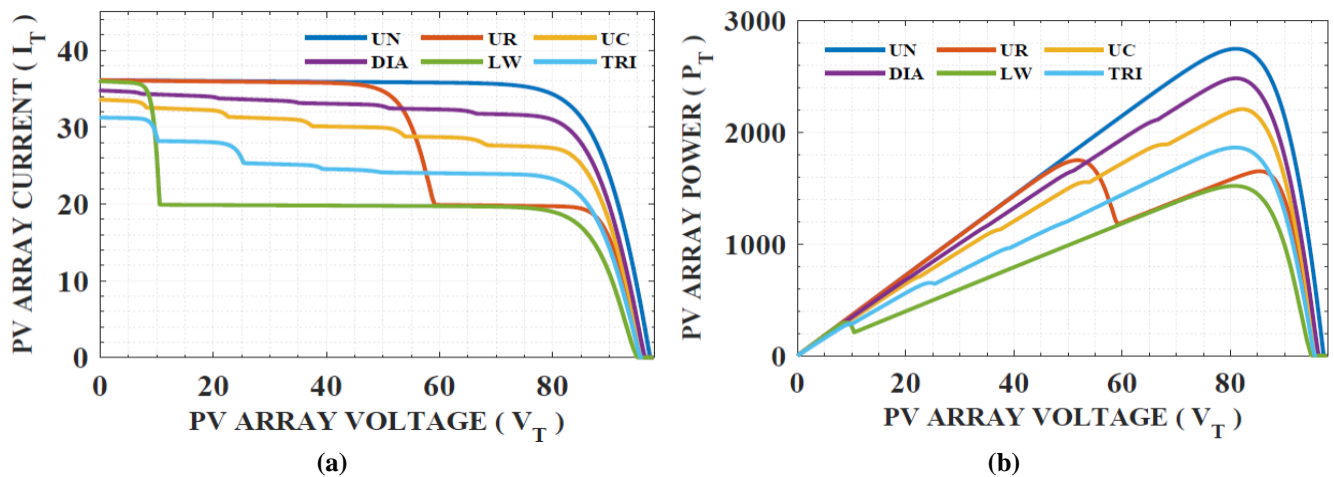
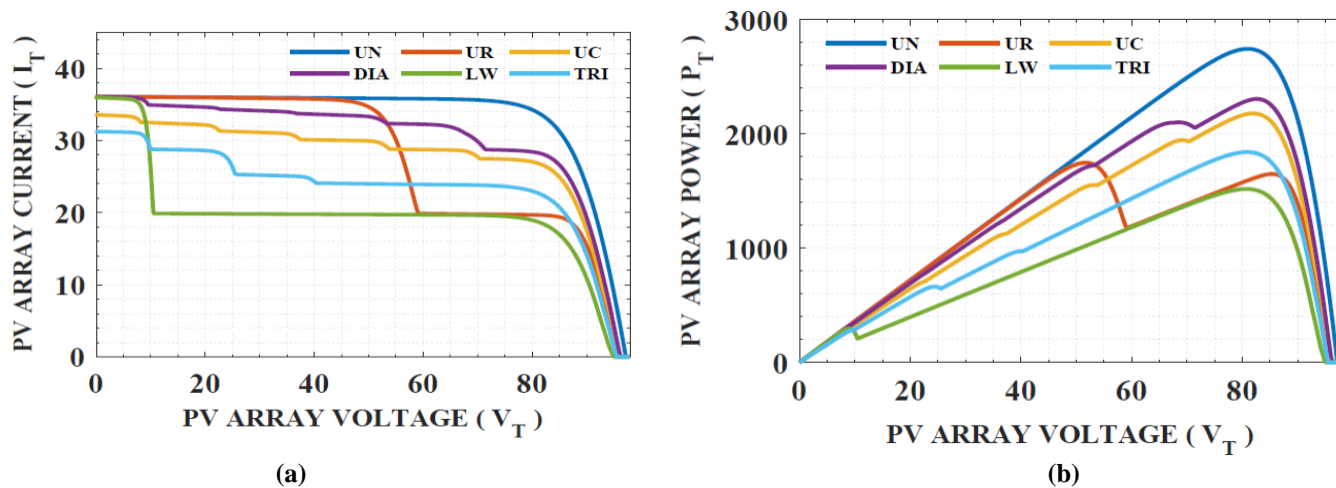**Fig. 4.** (a) Array Current Curve (b) Array Power Curve of BLTCT Configuration

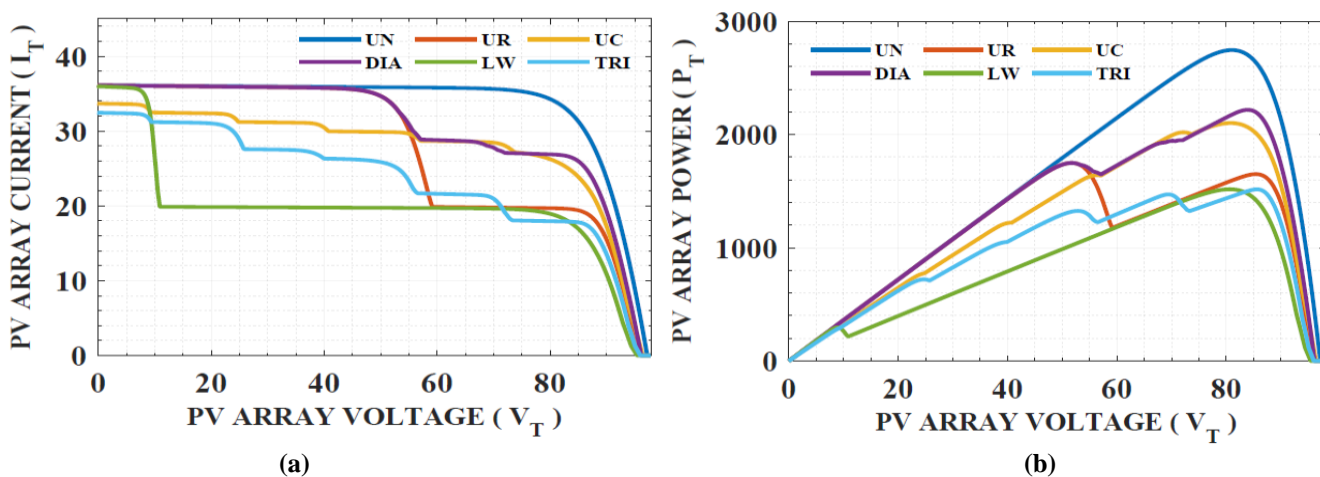**Fig. 5.** (a) Array Current Curve (b) Array Power Curve of HCTCT Configuration

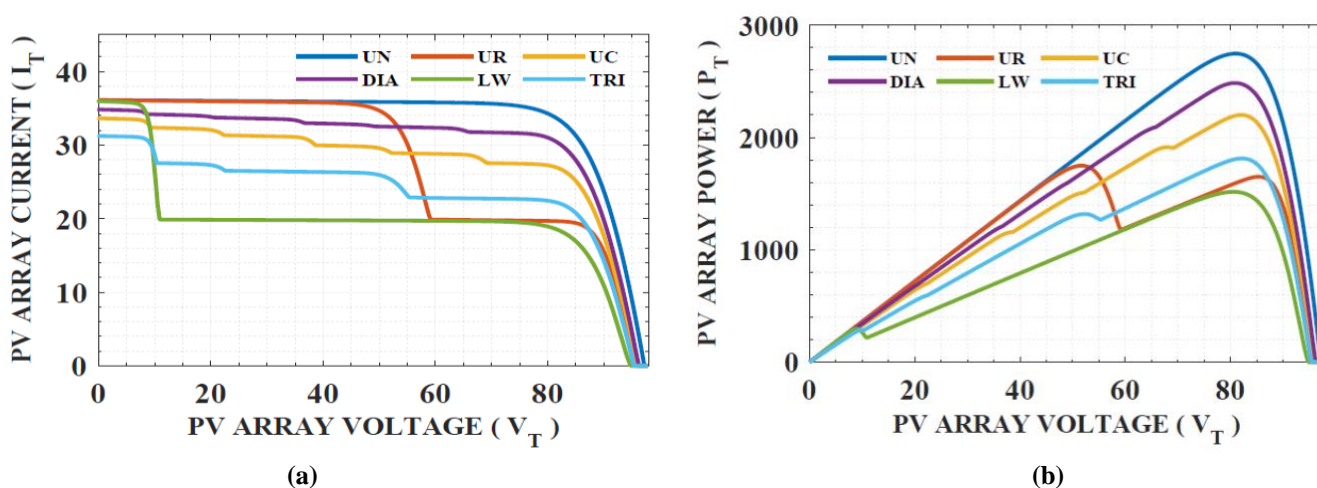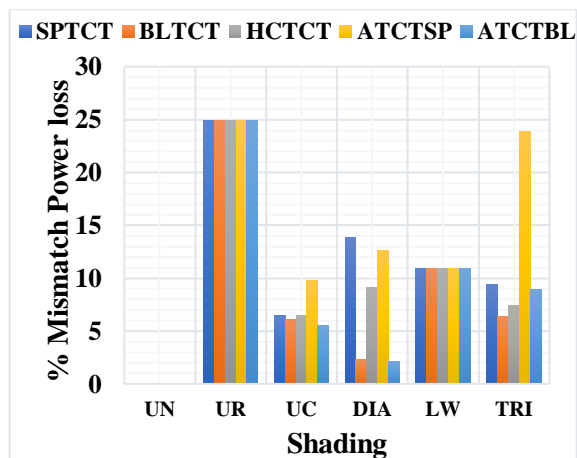**Fig. 6.** (a) Array Current Curve (b) Array Power Curve of ATCTSP Configuration
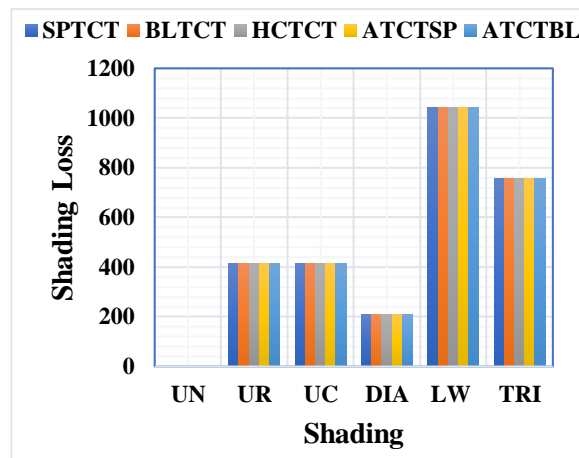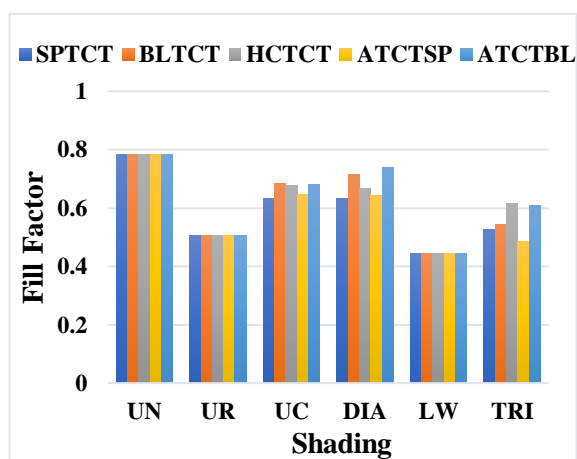

Fig. 7. (a) Array Current Curve (b) Array Power Curve of ATCTBL Configuration
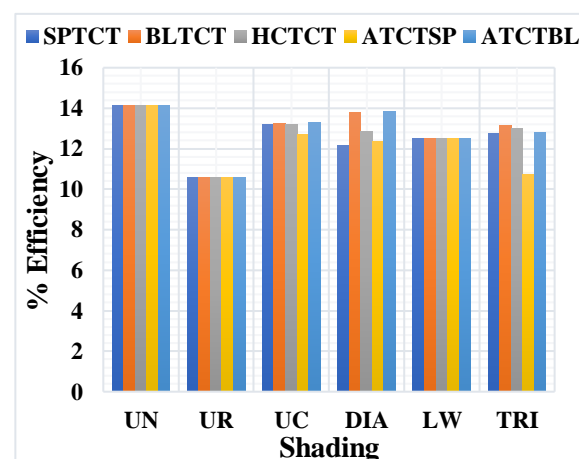
(a)

(b)

(c)

(d)

Fig. 8. Comparative Analysis of Hybrid PV Array Configurations (a) Shading Loss (b) % Mismatch Loss (c) Fill-Factor (d) % Efficiency

3.1 Payback Time Assessment of ATCTBL Configuration For Diagonal Shading

The generated power in SPTCT = 2187 W

The generated power in ATCTBL = 2484 W

$$\% \text{ Power gain} = \frac{((P_{max})_{ATCTBL} - (P_{max})_{SPTCT})}{(P_{max})_{SPTCT}} \times 100$$
$$= 13.58\%.$$

In a day, assume duration of partial shading = 4 Hrs, then Power saving per day = (2484 – 2187) * 4 = 1.188 Kwh. Then, total units saved per annum ≈ 434 Kwh = 434 units.

Compared to SPTCT topology, ATCTBL requires 4 additional wires for 6 x 6 array. Consider the length of one wire is 2 ft, then total required wired length is 8 ft and cost of one wire is taken as 1 $. Therefore, total cost needed for ATCTBL configuration is 8 $.

Similarly, cost per unit is considered as 0.107 $, then total units saved = 0.107 * 434 =46.4 $.

$$\text{Payback time in a year} = \frac{8}{46.4} = 2 \text{ months}$$

Cost study shows that just 4 more ATCTBL connections are needed to mitigate partial shading. Four extra connections cost $8 more than SPTCT. Within 2 months of a year, a solar PV array with a 25-year lifespan returns more power than a SPTCT array with diagonal shading and Table 9 shows payback time of ATCTBL hybrid configurations as compared to others.

Table 9 Payback time of ATCTBL Hybrid configuration

Shading Scheme	Configuration	% Power gain	Payback Period
	SPTCT	13.58	2 months
Diagonal	BLTCT	0.16	No additional cost needed
	HCTCT	7.67	1 month
	ASPTCT	12	2.3 months

4. Conclusion

This paper analyses the various hybrid topologies under PSC. From the analysis the following observations are made.

1. Under UR and LW Shading conditions, all configurations give same response with a shade dispersion factor of 33.33% and 83.33% respectively.
2. For UC shading, ATCTBL generates global maximum power of 2200 W, followed by BLTCT, HCTCT, SPTCT and ATCTSP configurations with a shade dispersion factor of 33.33% distributed in entire String length of first two columns. In addition to this, it produces lowest mismatch power loss of 5.56%, optimum Fill-factor and efficiency of 0.68 and 13.31 respectively.
3. Under DIA shading condition, ATCTBL produces maximum power of 2484 W, lowest mismatch power loss of 2.12%, optimum Fill-factor and efficiency of 0.74 and 13.81 respectively, followed by BLTCT, HCTCT, SPTCT and ATCTSP configurations with a shade dispersion factor of 16.66%.
4. For TRI shading scheme, BLTCT generates maximum power of 1863 W followed by HCTCT, ATCTBL, SPTCT and ATCTSP with a shade dispersion factor of 58.33 %.

Finally, it was confirmed that a decrease in mismatch power loss or the presence of fewer series connections between the modules can boost a PV array's maximum power capability. Based on peak power points and shading factor, this research helps design PV module interconnections in congested locations. Furthermore, the best fill factor is achieved when shade is dispersed across the entire string rather than focused in a single location. Finally, the configuration of a PV array, as well as the shading pattern and placement, each play a major role in its efficiency. Among all, ATCTBL gives best response in most of the shading schemes. Because of more inter connections between the panels it offers high initial cost, but it is recovered within 2 months only.

References

[1] H. Oufettoul, S. Motahhir, G. Aniba, M. Masud, and M.A AlZain, "Improved TCT topology for shaded photovoltaic arrays", Energy Reports, vol.8, pp.5943-5956, 2022.

[2] A.S Yadav, and V. Mukherjee, "Conventional and advanced PV array configurations to extract maximum power under partial shading conditions: A review", Renewable Energy, vol.178, pp.977-1005, 2021.

[3] P.R Satpathy, T.S Babu, A.H Mahmoud, R. Sharma, and B. Nastasi, "A TCT-SC hybridized voltage equalizer for partial shading mitigation in PV arrays", IEEE Transactions on Sustainable Energy, vol. 4, pp.2268-2281, 2021.

[4] K. Abdulmawjood, S. Alsadi, S.S Refaat, and W.G Morsi, "Characteristic study of solar photovoltaic array under different partial shading conditions" IEEE Access, vol.10, pp.6856-6866, 2021.

[5] A.S.A Elgharbawy, Ali, "Review on corrosion in solar panels", International Journal of Smart Grid-ijSmartGrid 2, vol. 4, pp. 218-220, Dec 2018.

[6] J. Solis, A. Råberg, J. André, and M. Nilsson, "Analyzing the effect of snow in PV regulator response in a PV solar park", International Conference on Smart Grid (icSmartGrid), pp. 72-75. IEEE, Jun 2021.

[7] S. Silvestre, A. Boronat, and A. Chouder, "Study of bypass diodes configuration on PV modules" applied energy, vol .9, pp.1632-1640, 2009.

[8] G.Petrone, G. Spagnuolo, R. Teodorescu, M. Veerachary, and M. Vitelli, "Reliability issues in photovoltaic power

processing systems" IEEE transactions on Industrial Electronics, vol. 7, pp.2569-2580, 2008.

[9] B.N Alajmi, K.H Ahmed, S.J Finney and B.W Williams, "A maximum power point tracking technique for partially shaded photovoltaic systems in microgrids" IEEE transactions on Industrial Electronics, vol. 4, pp.1596-1606, 2011.

[10] J.I Corcau, and L. Dinca, "Modeling and analysis of a fuzzy type MPPT algorithm" International Conference on Electrical Drives & Power Electronics (EDPE), pp. 230-234, IEEE, Sept 2019.

[11] S. Messalti, A. Harrag, and A. Loukriz, "A new variable step size neural networks MPPT controller: Review, simulation and hardware implementation" Renewable and Sustainable Energy Reviews, vol. 68, pp.221-233, 2017.

[12] M. Sarvi, S. Ahmadi, and S. Abdi, "A PSO-based maximum power point tracking for photovoltaic systems under environmental and partially shaded conditions", Progress in Photovoltaics: Research and Applications, vol. 2, pp.201-214, 2015.

[13] H. Zheng, R. Challoo, and J. Proano, "Shading and bypass diode impacts to energy extraction of PV arrays under different converter configurations", Renewable Energy, vol. 68, pp.58-66, 2014.

[14] A. Bidram, A. Davoudi, and R.S Balog, "Control and circuit techniques to mitigate partial shading effects in photovoltaic arrays" IEEE Journal of Photovoltaics, vol. 4, pp.532-546, 2012.

[15] O. Bingöl, and B. Özkaya, "Analysis and comparison of different PV array configurations under partial shading conditions" Solar Energy, vol. 160, pp.336-343, 2018.

[16] S. Mohammadnejad, A. Khalafi, and S.M Ahmadi, "Mathematical analysis of total-cross-tied photovoltaic array under partial shading condition and its comparison with other configurations", Solar energy, vol. 133, pp.501-511, 2016.

[17] M. Premkumar, U. Subramaniam, T.S Babu, R.M Elavarasan, and L. Mihet-Popa, "Evaluation of mathematical model to characterize the performance of conventional and hybrid PV array topologies under static and dynamic shading patterns", Energies, vol. 12, pp.3216, 2020.

[18] K. Abdulmawjood, S. Alsadi, S.S Refaat, and W.G Morsi, "Characteristic study of solar photovoltaic array under different partial shading conditions", IEEE Access, vol. 10, pp.6856-6866, 2022.

[19] M. Etarhouni, B. Chong, and L. Zhang, "A novel square algorithm for maximising the output power from a partially shaded photovoltaic array system" Optik, vol. 257, pp.168-187, 2022.

[20] H. N. Suresh, S. Rajanna, S. B. Thanikanti, and H. H. Alhelou, "Hybrid interconnection schemes for output power enhancement of solar photovoltaic array under partial shading conditions," IET Renewable Power Generation, vol. 16, no. 13, pp. 2859-2880, 2022.

[21] B.s.s Santosh, M.M.T Ansari , P. Kantarao, and G. Kusuma, "Power loss analysis of Traditional PV array Configurations under different shading conditions", International Journal of Renewable Energy Research (IJRER), vol.12(2), pp.1176-1203, 2022.